

Toward PZ summation without Z

Ettore Biondi and Stewart A. Levin

ABSTRACT

We examine the possibility of separating up-going and down-going wavefields of ocean-bottom data using only one component. This possibility relies on differential static shifts of the up-going events caused by near sea-bottom inhomogeneities. We downward continue a survey to the sea bottom to recover these shifts while leaving nonprimary arrivals smoothly curved. We then explore whether or not these static shifts are detectable in the curvelet domain. In addition, we show how suppressing fine-scale curvelet coefficients affects an event distributed along a disrupted hyperbolic curve. From our synthetic examples, we demonstrate that the curvelet domain has the potential to separate up-going from down-going events.

INTRODUCTION

The separation of up-going and down-going waves of a multicomponent dataset is one of the fundamental preprocessing steps in ocean-bottom acquisition (OBN) (Grion, 2010). This wavefield decomposition is usually performed by summing the pressure (P) and vertical velocity (V_z) components (Schalkwijk et al., 1999), a process commonly known as ‘PZ summation’. Before summing the two components, the difference in instrument coupling response between the geophone and hydrophone must be properly accounted for by applying a calibration filter to the recorded vertical velocity (Melbø et al., 2002; Biondi and Levin, 2014).

Many applications have already demonstrated the advantages and the importance of such wavefield separation. For example, water reverberations can be attenuated by using the extracted up-going events (Rosales and Guitton, 2004). Furthermore, a source wavelet can be easily estimated from the down-going separated direct arrival (Wong and Ronen, 2009). In addition, the combined information of the two wavefields can be used in the context of improving the images obtained by least-squares reverse-time migration (LSRTM) (Wong et al., 2010).

Current up-down wavefield separation techniques rely on the assumption that the data contain noise-free up- and down-going events. However, it is well known that the vertical velocity component can be contaminated by shear wave energy (Paffenholz et al., 2006), a phenomenon commonly called V_z noise. The leakage of shear energy into the vertical velocity, which is not recorded by hydrophones, can degrade PZ summation results and subsequent imaging (Campman et al., 2005). Different

techniques have been proposed to suppress or dampen the effect of Vz noise present in the vertical component (Shatilo et al., 2004). We discuss how the up-down wavefield separation may be performed using only the pressure field of the recorded data. We start by explaining the main assumption, seafloor statics, on which this single component separation relies. We show that by downward continuing a survey line to the sea bottom we can retrieve the static shifts of the up-going events caused by the near sea-bottom inhomogeneities. We then briefly review the curvelet transform and apply this transformation to two hyperbolic events, one of which is affected by static shifts. We show the differences between these events in the curvelet domain. The possibility of separating up- and down-going energy without the combination of the pressure and vertical components can enable application of the wavefield separation to the horizontal components as well.

UP-GOING AND DOWN-GOING STATIC DIFFERENCES

We recall the concept of wavefield focusing shown by Claerbout (1976) to explain why up-going events should exhibit static shifts not present on the down-going arrivals after downward continuation of the survey to the sea bottom. Consider a wavefront that has been disrupted by small-scale inhomogeneities present in the subsurface. When this wavefront propagates through a homogeneous medium (e.g., a water layer), the wavefront heals and the energy spreads out smoothly. The longer the wave propagates through the homogeneous medium, the more it will heal.

We start with the layered earth model shown in Figure 1a. This figure displays a reciprocal ocean-bottom acquisition scenario where the shots and receiver are on the sea bottom. The black arrow indicates a primary event that we would record with this survey. The recorded reflection is disrupted by the near sea-floor variations as we see in the common-shot gather of Figure 1b. We then upward continue the receivers to the sea surface (Figure 2a) to simulate the physical reciprocal experiment of an OBN acquisition. The red and green arrows in this figure indicate the direct arrival and its first-order surface related multiple respectively, which are not affected by the near sea-bottom inhomogeneities. Figure 2b displays the common-shot gather of these events and the upward continued primary reflection. Ignoring the minor artifact introduced by the upward continuation, we note that the static shifts present on the primary event are eliminated, and the energy is distributed along a smooth hyperbolic curve. This effect comes as a result of wavefront healing as the wave propagates through the homogeneous water layer.

Now, if we downward continue the gather shown in Figure 2b, we expect to focus the energy of the direct event at the source location and at zero time, and also start collapsing the energy of the other events (Figure 3a). This is indeed what we see in the downward continued gather of Figure 3b. In fact, the energy of the direct event is tightly focused, and the two other events have started focusing. The main point to note is that the static shifts, initially present in the primary reflection, have been retrieved by sinking the receivers to the sea floor. In contrast, the energy of the other

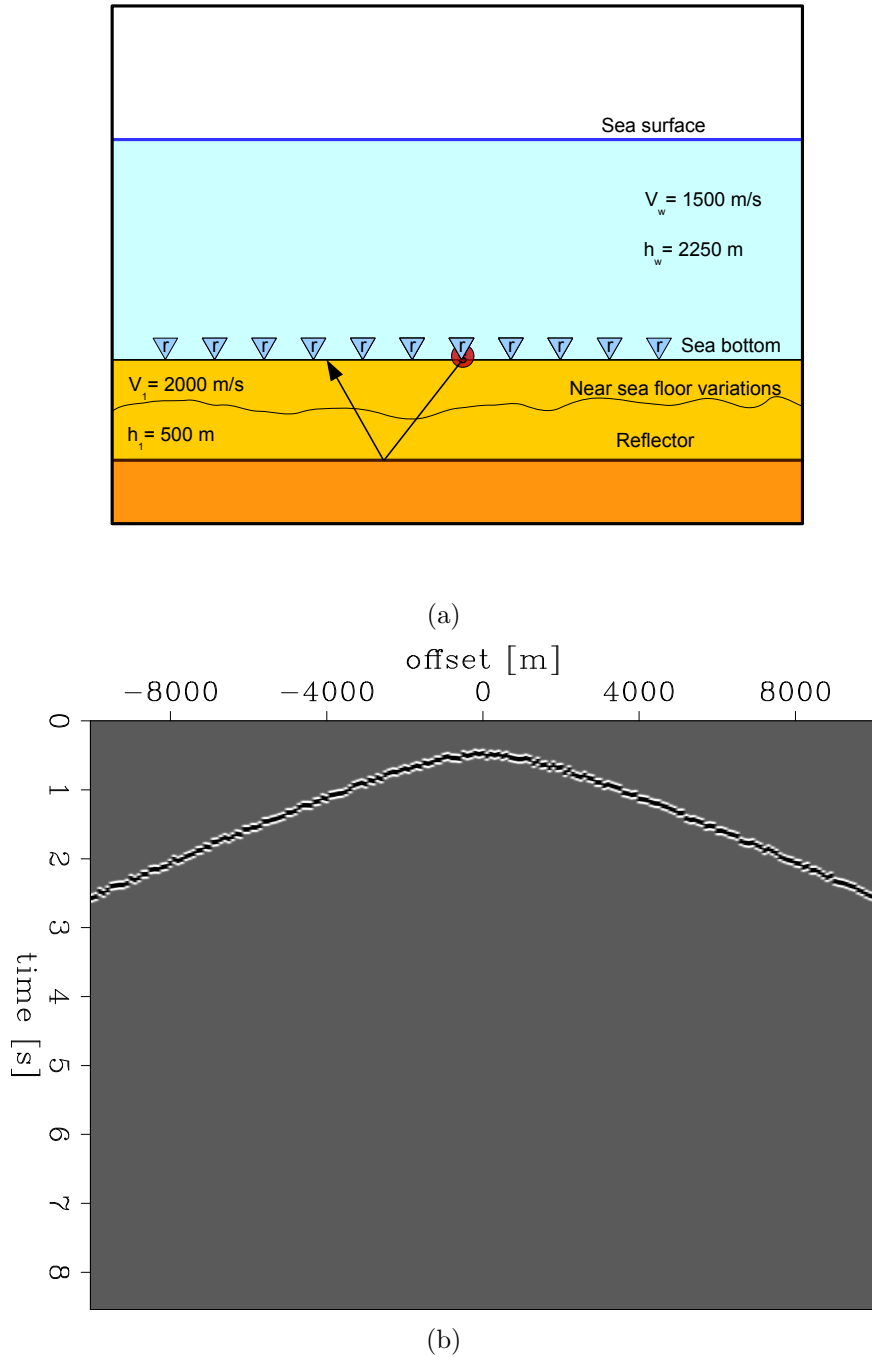


Figure 1: Initial acquisition setting with source and receivers at the sea bottom. (a) Earth model used for generating one up-going event displayed by the black arrow. [NR](b) Single up-going event recorded at the sea floor. The effect of the near sea-floor variations are visible in the statics present in the hyperbolic event. [ER]

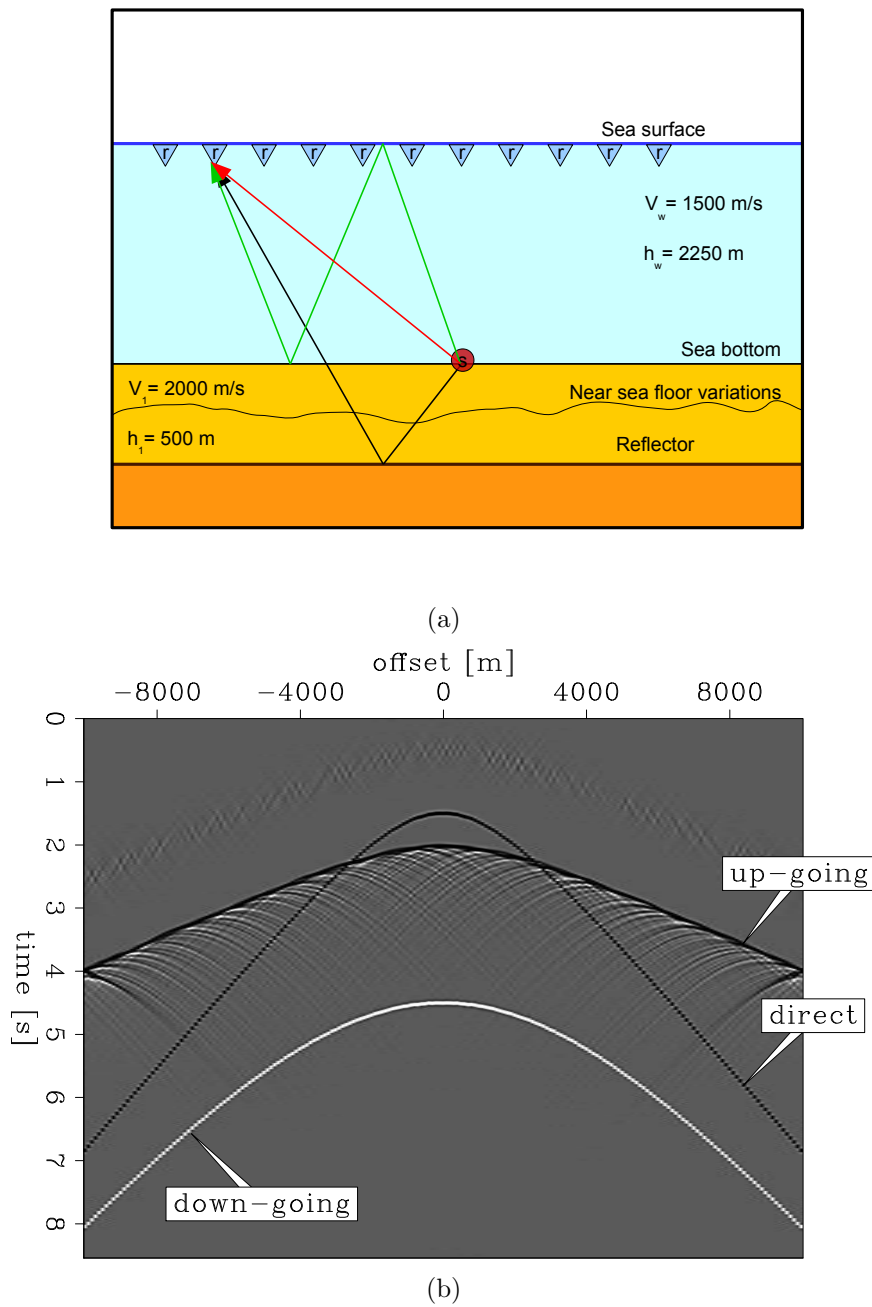


Figure 2: Events recorded when the receivers are at the sea surface. (a) Illustration of the recorded events. The red, green, and black arrows represent the direct arrival, its multiple, and the upward continue primary event, respectively. [NR](b) Common-shot gather showing the upward continue primary event, the direct arrival, and its first-order multiple. The statics present on the primary reflection of Figure 1b are eliminated by the propagation of the event toward the sea surface. Some artifacts of the upward continuation are also present. [ER]

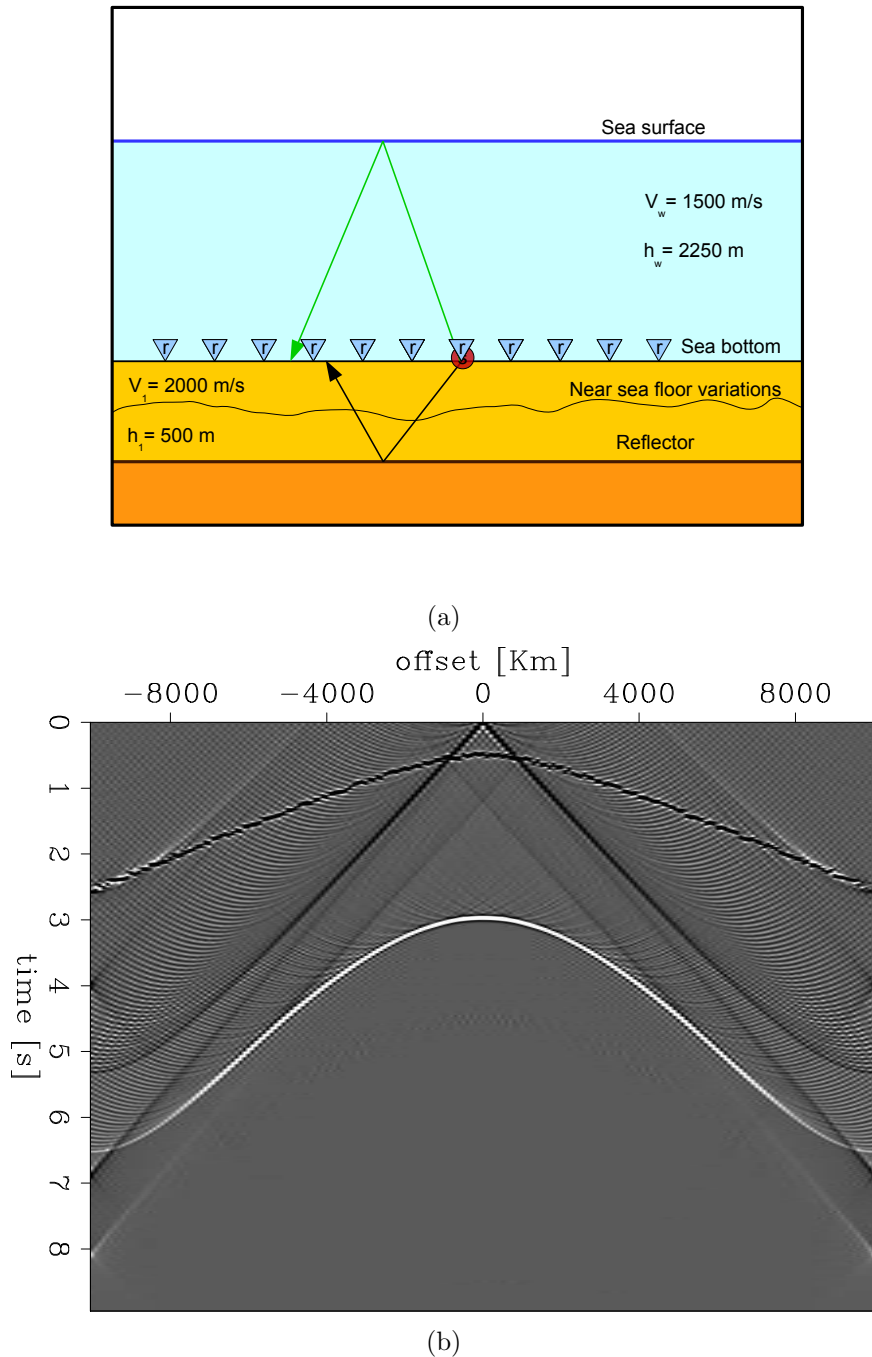


Figure 3: Downward continuation of the events shown in Figure 2. (a) Illustration of how the recorded events change when the receivers are downward continued to the sea-floor surface. [NR](b) Downward continued common-shot gather of Figure 2b. The direct event tends to focus at zero time; while, its multiple starts collapsing. The statics of up-going primary event are recovered when the receivers are downward continued to the same depth of the source. [ER]

down-going event is still distributed along smooth curves or lines.

This simple illustrative example shows that the difference in static shifts between the up-going and down-going events can be recovered by downward continuing the survey line to the sea floor. This difference is the key element on which our separation criterion relies.

THE CURVELET TRANSFORM

Before explaining how the curvelet transform can capture the differences between events disrupted by static shifts and arrivals distributed along smooth curves, we briefly show the basic concept behind the curvelet transform. The curvelet domain was originally developed in the context of image processing, and it has been widely used for image denoising (Starck et al., 2002; Candés et al., 2006). This transform has also been applied to seismic imaging to attenuate the effect of Vz noise on the PZ summation results (Peng et al., 2013).

The main idea of the curvelet transform is to take an original signal $f(x)$, usually an image, and decompose into it a sum of wavelets $\varphi_{j,l,k}(x)$ with a different j scale, l orientation, and k position,

$$f(x) = \sum_{j,l,k} c(j, l, k) \varphi_{j,l,k}(x), \quad (1)$$

where $c(j, l, k)$ coefficients are given by the scalar product of the original signal with the basis functions

$$c(j, l, k) = \langle f, \varphi_{j,l,k} \rangle = \int f(x) \varphi_{j,l,k}(x) dx. \quad (2)$$

Figure 6 shows the curvelet transform flowchart by Starck et al. (2002). The image is divided into a different number of blocks for each scale. As the level of the detail that we want to represent increases, the number of blocks increases as well. At first, we take the whole image and apply a wavelet transform. Then, we divide the image into a fixed number of blocks, and apply the wavelet transform on each section. This process continues until we reach the desired number of scales. The wavelet transform is performed as a combination of Fourier and Radon transforms followed by a ridgelet transform along lines in the Radon domain. All the mathematical details can be found in Starck et al. (2002). The ability of the curvelet transform to analyze different level of details on an image, thanks to the inclusion of the j scale factor in the wavelet expansion, enables us to capture the difference between events disrupted by static shifts and events unaffected by them as we see in the next section.

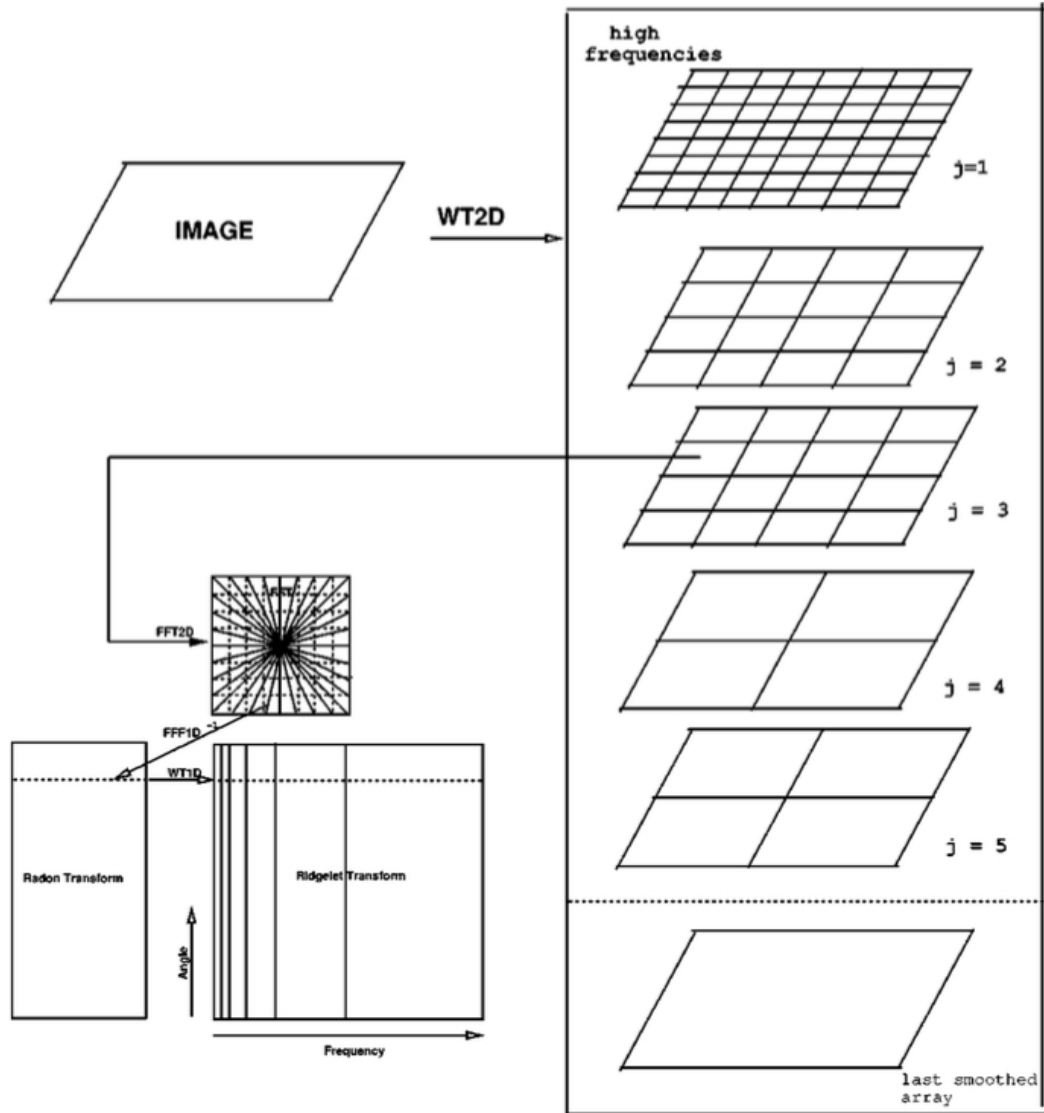


Figure 4: Figure from Starck et al. (2002). Graphical explanation of the curvelet transform. An input image is decomposed into a different number of blocks as a function of the scale to be analyzed. The wavelet/ridgelet transform is then applied to each block. [NR]

THE EFFECT OF STATICS IN THE CURVELET DOMAIN

In this section, we show the differences of two hyperbolic events in the curvelet domain, one disrupted by static shifts and one unaffected by static shifts. Figure 5 displays these two hyperbolic events. The left panel shows the down-going sea-bottom multiple event, which is unaffected by statics. The right panel depicts the up-going reflection event with static shifts resulting from the near sea-floor variations.

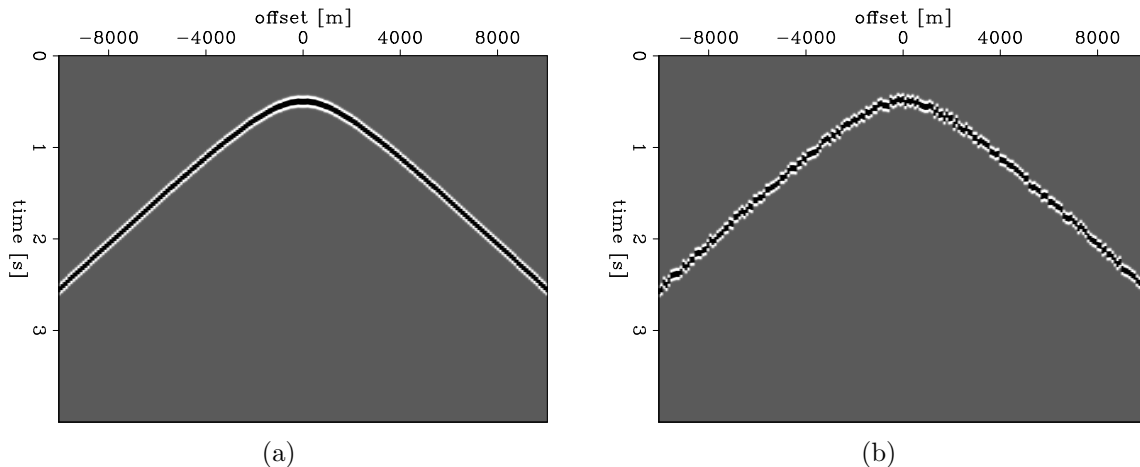
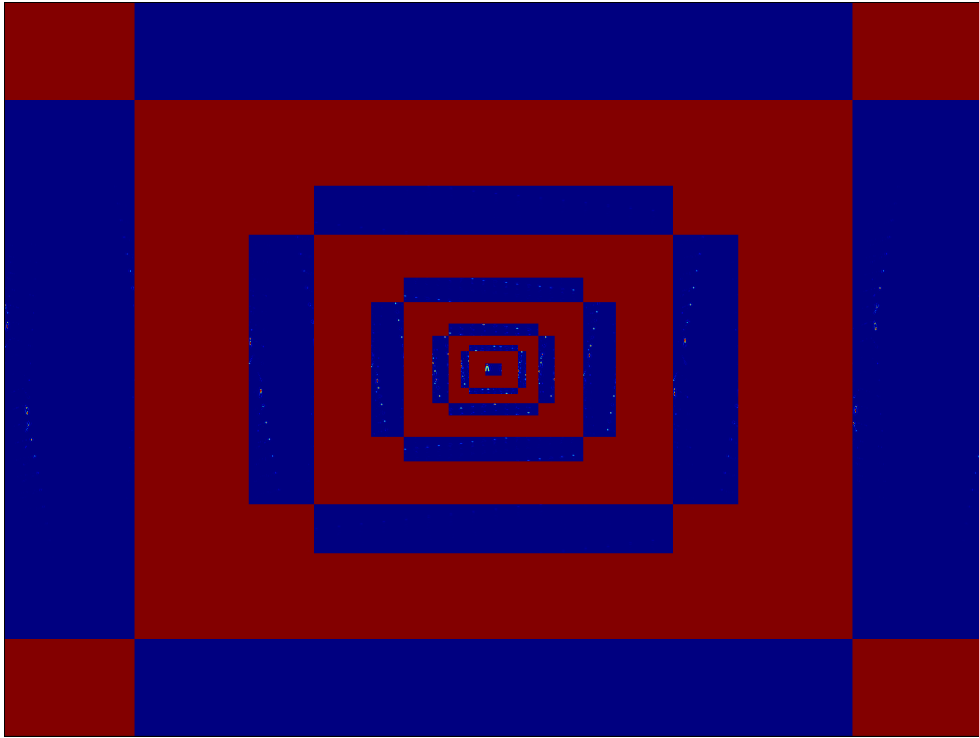


Figure 5: Hyperbolic events used for analyzing apparent differences in the curvelet domain. (a) Event with no static shifts. (b) Event affected by statics. [ER]

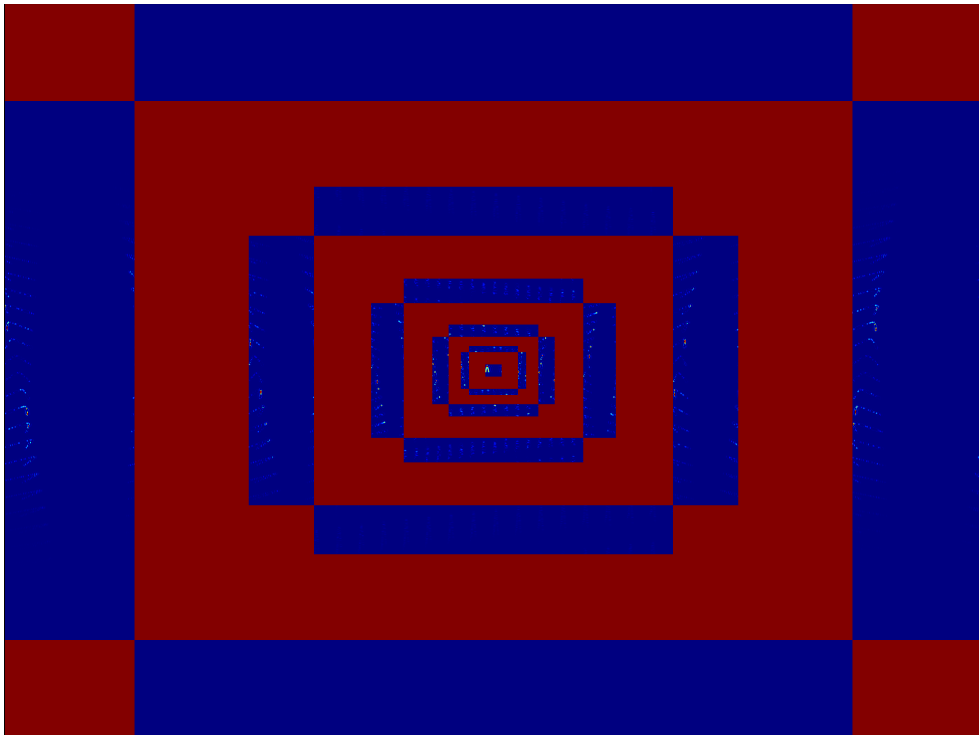
By applying the curvelet transform described in the previous section, we obtain the panels of Figure 6. These images display the coefficients of the curvelets necessary to represent the original functions. The central square panel represents the coefficients of the curvelets of the whole image scale. The surrounding red zone is present just to separate the coefficients from one scale to another. The next four surrounding blue rectangles are the coefficients of the curvelets of a finer scale. As we move to the external rectangles, we find the multiplicative factors of finer scale curvelets. Comparing the curvelet transform factors of the two events, we observe that the finer scale coefficients are more scattered for the hyperbola with static shifts (Figure 6b) than for the hyperbola with no static shifts (Figure 6a).

The same conclusion can be drawn from the closeups of the central curvelet domain coefficients, shown in Figure 7. However, from these closeups it is apparent that at a coarse scale, the two events are similar. The scattering behavior of the fine scale coefficients of the disrupted hyperbolic event can be a distinctive factor that enables us to separate up-going energy from down-going arrivals, after the downward continuation of the survey line.

In the following synthetic example, we show how to employ the curvelet domain to separate the two hyperbolic events, one with statics and one without them. Figure 8(a) shows the gather containing these two events, and Figure 8(b) is the curvelet

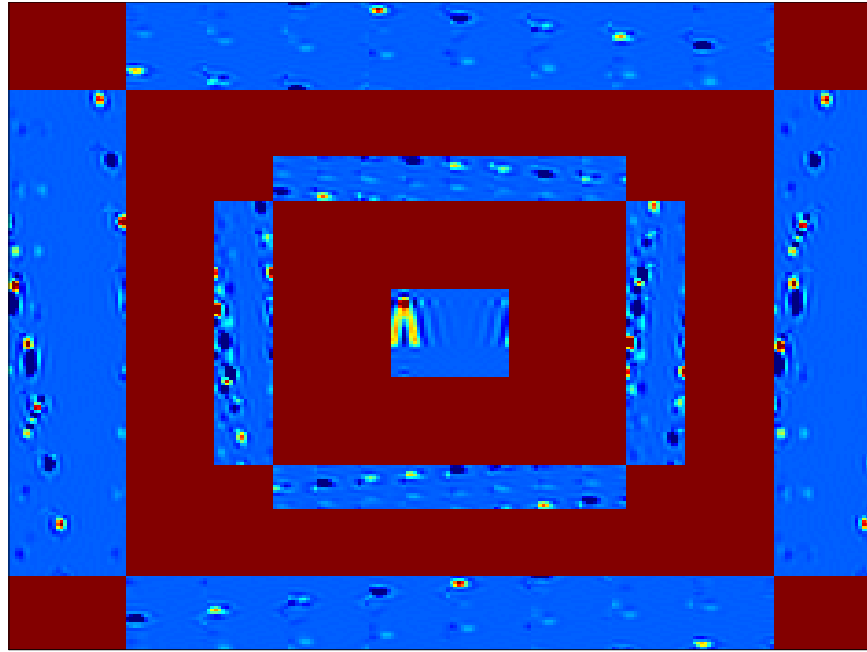


(a)

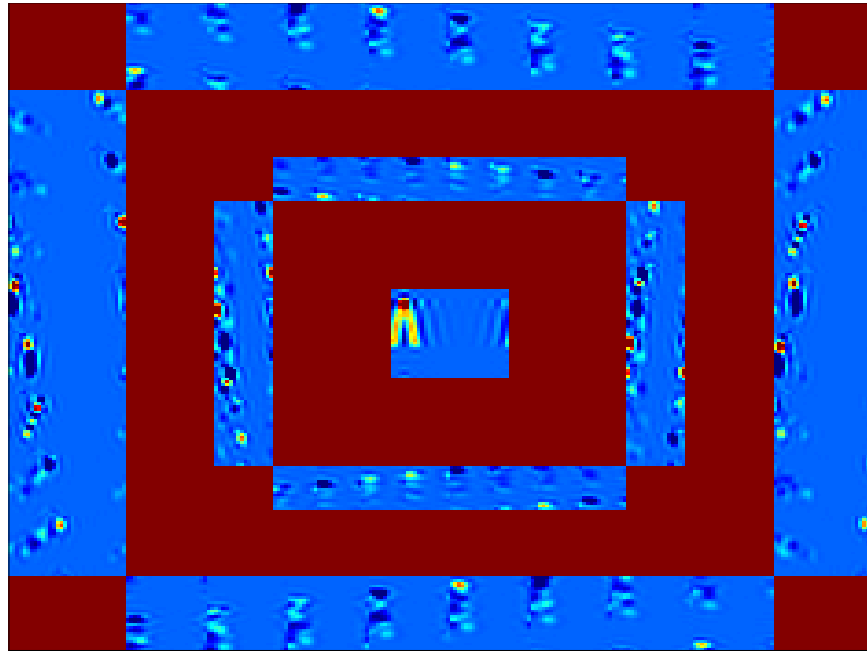


(b)

Figure 6: Curvelet domain coefficients of the hyperbolic events of Figure 5. (a) Coefficients of static-free event. (b) Coefficients of event affected by statics. As we look toward finer scale factors (external blue rectangles), the coefficients of the disrupted event become more scattered. **[ER]**

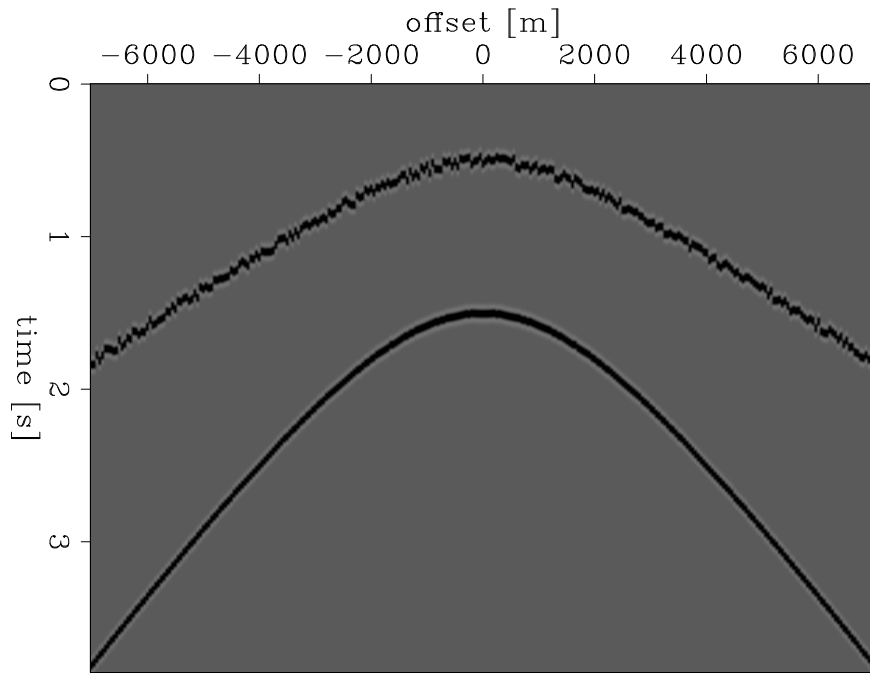


(a)

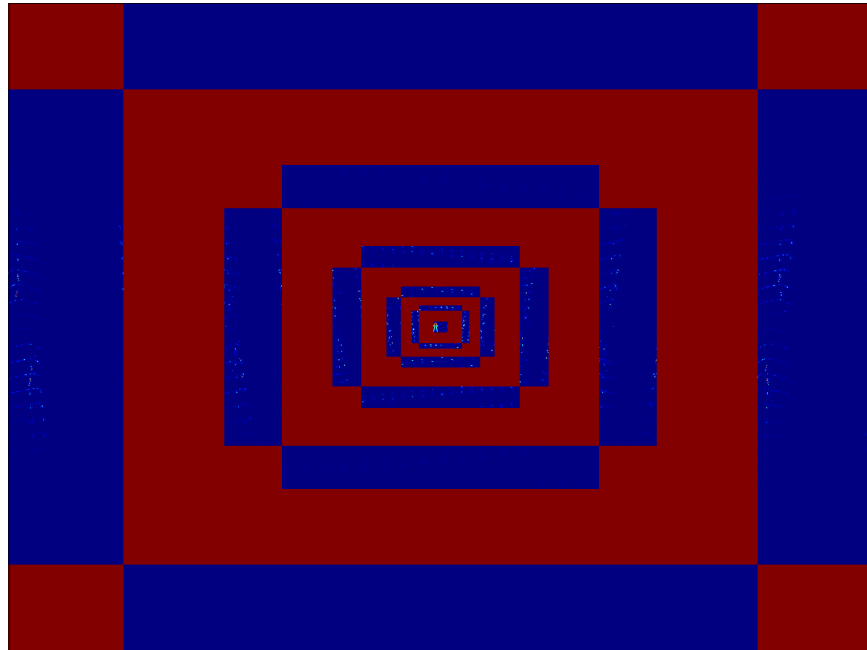


(b)

Figure 7: Closeups of the first three scales of the curvelet transform factors of Figure 6. (a) Closeup of curvelet factors of static-free event. (b) Closeup of curvelet factors of event affected by statics. Comparing the whole image scale curvelet factors, we note that the two images are similar. However, as we move to finer scale factors, the coefficients for the disrupted event tend to become less concentrated on a single area. [ER]



(a)



(b)

Figure 8: Synthetic example for explaining how to separate an event affected by statics from an event unaffected by them. (a) Gather with the two hyperbolic events. (b) Curvelet domain representation of the two events. The scattered coefficients at fine scales represent the amplitudes of the curvelets of the event disrupted by the static shifts. [ER]

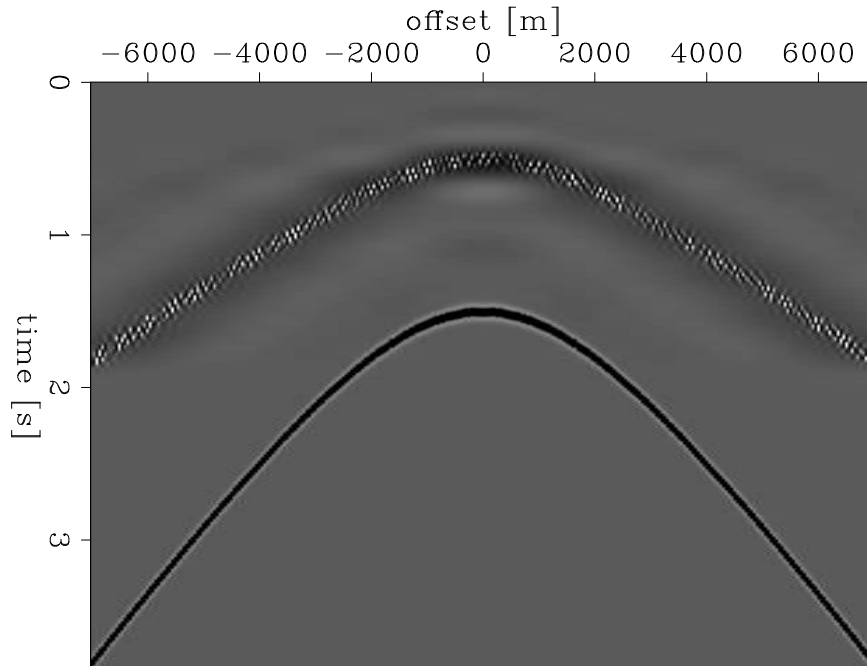


Figure 9: Resulting gather after filtering out the fine-scale curvelet coefficients of the event affected by statics. The event distributed along the smooth hyperbola is completely reconstructed. The hyperbolic trend of the event with statics can still be seen, but its energy now appears as random noise. [ER]

domain representation of the gather. From the previous observations, we can say that the curvelet domain coefficients of the event with statics are more dispersed than the ones for the smooth hyperbolic event (Figure 6b). Figure 9 is the result of filtering the scattered coefficients of the last four fine curvelet scales and applying the inverse curvelet transform. Observe that we are able to correctly reconstruct the static-free event, and make the disrupted event more similar to random noise distributed along a hyperbolic curve. This random energy can be then attenuated by applying a denoising technique (Kahoo and Siahkoochi, 2009; Han et al., 2014), and thus separating the two events.

FUTURE WORKS AND CONCLUSIONS

Performing a wavefield up-down separation by using just one component of a multi-component ocean bottom dataset is an attractive goal, especially when PZ summation algorithms fail because of the presence of V_z noise in the recorded vertical velocity. We discussed the possibility of doing up-down wavefield separation by downward continuing the survey line to the ocean bottom, and then separating up- and down-going energy in the curvelet domain. We explained how to retrieve the static shifts caused by near sea-floor inhomogeneities that affect up-going events by downward continuation. We observe that the curvelet domain is able to capture the differences between

events affected by statics and events without them. We have also shown that by suppressing the fine scale curvelets coefficients of the disrupted event, we were able to make this event appear as a random noise feature, making it easier to filter it out with denoising techniques. This example demonstrates that the curvelet domain has the potential to separate up-going events from down-going ones. In the future, we will use these observations to separate up-going energy from down-going events, both on a more complex synthetic gather and a real common-receiver gather of an OBN dataset. Furthermore, because this wavefield decomposition is based on a single component, we will be able to apply this curvelet domain separation on the pressure and vertical components geophone components separately, and possibly also on the horizontal geophone components.

REFERENCES

- Biondi, E. and S. A. Levin, 2014, Application of the up-down separation using PZ calibration filter based on critically refracted waves.
- Campman, X. H., K. van Wijk, J. A. Scales, , and G. C. Herman, 2005, Imaging and suppressing near-receiver scattered surface waves: *Geophysics*, **70**, no. 2, V21–V29.
- Candés, E., L. Demanet, D. Donoho, and L. Ying, 2006, Fast discrete curvelet transforms: *Multiscale Modeling & Simulation*, **5**, 861–899.
- Claerbout, J. F., 1976, *Fundamentals of Geophysical Data Processing*: Blackwell Scientific Publications.
- Grion, S., 2010, From PZ Sum to wavefield separation, mirror imaging and up down deconvolution: *The Evolution of OBS Data Processing: Annual International Meeting*, *KazGeo*, 83–87.
- Han, L., M. D. Sacchi, and L. Han, 2014, Spectral decomposition and de-noising via time-frequency and space-wavenumber reassignment: *Geophysical Prospecting*, **62**, 244–257.
- Kahoo, A. R. and H. R. Siahkoobi, 2009, Random noise suppression from seismic data using time-frequency peak filtering: *Annual International Meeting*, 71st EAGE Conference and Exhibition, P317.
- Melbø A. H. S., J. O. A. Robertsson, and D. Manen, 2002, PZ calibration by applying the equation of motion to critically refracted waves, 2002 SEG Annual Meeting, 1030–1033. Society of Exploration Geophysicists.
- Paffenholz, J., R. Shurtleff, D. Hays, and P. Docherty, 2006, Shear wave noise on OBS Vz Data - Part I Evidence from field data: *Annual International Meeting*, 68th EAGE Conference and Exhibition, B046.
- Peng, C., R. Huang, and B. Asmerom, 2013, Shear noise attenuation and PZ matching for OBN data with a new scheme of complex wavelet transform: *Annual International Meeting*, 75th EAGE Conference and Exhibition, Tu 02 07, 250–254.
- Rosales, D. A. and A. Guitton, 2004, Ocean-bottom hydrophone and geophone coupling.
- Schalkwijk, K. M., C. P. A. Wapenaar, and D. J. Verschuur, 1999, Application of two-step decomposition to multicomponent ocean-bottom data: *Theory and case*

- study: *Journal of Seismic Exploration*, **8**, 261–278.
- Shatilo, A., R. Duren, and T. Rape, 2004, Effect of noise suppression on quality of 2C OBC Image: Annual International Meeting, 2004 SEG Annual Meeting,, 917–920.
- Starck, J.-L., E. J. Candés, and D. L. Donoho, 2002, The curvelet transform for image denoising: *IEEE Transactions on Image Processing*, **11**, 670–684.
- Wong, M., B. Biondi, and S. Ronen, 2010, Joint least-squares inversion of up- and down-going signal for ocean bottom data sets.
- Wong, M. and S. Ronen, 2009, Source signature and static shifts estimations for multi-component ocean bottom data.